Semiconductor Physics, Quantum Electronics & Optoelectronics, 2009. V. 12, N 1. P. 72-76.

PACS 81.05.Hd, 81.05.Ys, 81.10.Dn

$Bi_2Te_{3-x}Se_x$ ⟨Ag⟩ (x = 0.04) nanocrystal formation

F.K. Aleskerov[1], S.K. Kahramanov[1], M.M. Asadov[2,*], K.S. Kahramanov[1]
[1]*Production Association, Azerbaijan National Academy of Sciences*
[2]*Institute of Chemical Problems, Azerbaijan National Academy of Sciences*
AZ 1143 Baku, G. Javid av., 29
[*]*E-mail: mirasadov@yandex.ru; mirasadov@gmail.com*

Abstract. The results of experimental researches dealing with formation of nanometric-size doped (Ag) layers on the surface (0001) between $Te^{(1)}$–$Te^{(1)}$ telluride quintet layers in $Bi_2Te_{3-x}Se_x$⟨Ag⟩ (x = 0.04) crystals under directed crystallization has been submitted. During the crystal growth as result of impurity diffusion along a surface (0001), accumulation, redistribution and nanocrystal formation between $Te^{(1)}$–$Te^{(1)}$ layers occur. By the method of atomic-force microscopy, the $Bi_2Te_{3-x}Se_x$⟨Ag⟩ crystal images with nanolayers were obtained. Being based on experimental data, the fractal dimension of nanocrystalline layers was estimated.

Keywords: nanomaterial, low-dimensional structure, atomic-force microscopy.

Manuscript received 22.07.08; accepted for publication 18.12.08; published online 02.03.09.

1. Introduction

Fractal structures have a dimension incompatible with dimensionality of space where they exist. By a fractal cluster merging, the fractal surfaces can be formed. Those can be doped by formations between layers in layered crystals intercalated by the diffusion method. Such nanoformations can have a fractal structure. To explain the fractal structure, various models, subject to fractal aggregate formation features and experimental results, are used. The model of particle displacement process under action of random forces, which is a type of the Brownian movement, results in processes with fractal time. The plots of particle displacement dependence on time are fractal curves that can be used for description of diffusive growth of possible fractal formations. This situation occurs in real systems, for example, in nanoparticle formation inside $A_2^{V}B_3^{VI}$-type crystal layers [1].

The fractal time series of such quantities as layered deposits in various media and interlaminar formations in layered crystals can be estimated by the method of normalized swing [2]. These measurement sequences are characterized by the Hurst parameter *H*. The measurement record representing the fractal dimensional curve is characterized by $D = 2 - H$ equality.

For many time series, the observable natural normalized swing, i.e. dimensionless ratio R/S is well described by the empirical relation $R/S = (\tau/2)^H$, S – standard deviation, i.e., the square root of dispersion; R – swing, i.e., the difference between maximal and minimal accumulated natural observable inflow; τ – duration of selected time interval. In this case, the parameter *H* is symmetrically distributed around the average value 0.73 with a standard deviation 0.09. The value *H* for layered deposits is 0.74 and $H = 0.79$ for fractal "tree" rings.

Apart from methods of normal fractal Brownian function construction, there are also known ways of the Brownian surface and volume construction. For example, fractal Brownian curves obtained by the algorithm of sequential random additions of Voss [3] at different Hurst parameter *H* (0.9; 0.5; 0.1) values.

The fractal aggregates can also be formed inside interlaminar spaces of various layered crystals. Formed inside interlaminar space of $Te^{(1)}$–$Te^{(1)}$ telluride quintets of Bi_2Te_3 and Sb_2Te_3 crystals, the nanoparticles, according to [1], have fractality attributes. Results of studying the process of nanofractal "assemblage" formation in Bi_2Te_3-impurity system on $Bi_2Te_{3-x}Se_x$⟨Ag⟩ (x = 0.04) samples are submitted below.

2. Experimental techniques

The relief of assemblage surface of interlaminar nanofractals has been investigated using the method of atomic-force microscopy (AFM). To investigate spatial distributions of fractal nanoclusters, the discrete Fourier transform of cluster images was used.

The $Bi_2Te_{3-x}Se_x$⟨Ag⟩ (x = 0.04) system samples with impurities were grown by the method of vertically directed crystallization in graphitized quartz ampoules at 1000 K temperature with ~200 K/cm temperature

gradient; the velocity of crystallization zone travel was 1.2 cm/h. Using a scanning atomic-force microscope (mark NC-AFM), the relief of samples with nanofractal formations was investigated.

Pure surface preparation was implemented by a crystal cleavage of solid solutions of $Bi_2Te_3 - Bi_2Se_3$ system with impurities, along a plane (0001) on open-air right before investigation. Investigation of their surfaces was implemented by X-ray diffractometer and AFM images. The analysis showed the absence of harmful impurity content, in particular, oxygen in the obtained crystals. Specifically, the X-ray images argue presence of Ag, Ag_2Te, Ag_2Se, BiTe nanofragment traces on the $Bi_2Te_{3-x}Se_x\langle Ag\rangle$ (x = 0.04) crystal surface (0001) (Fig. 1).

After a special cutting, the samples have been cleaved. For cleavage, the knife of hard metallic alloy has been used.

3. Results and discussion

The experimental fact characterized by the perpendicular nanoparticle growth on a $Bi_2Te_{3-x}Se_x\langle Ag\rangle$ crystal plane (0001) has been revealed. The implemented AFM investigation of the $Bi_2Te_{3-x}Se_x\langle Ag\rangle$ surface (0001) relief in three-dimensional (3D) scale is represented in Fig. 2. The $Bi_2Te_{3-x}Se_x\langle Ag\rangle$ surface (0001) relief is given in Fig. 3. The AFM-image in 2D scale is represented in Fig. 4. On the right of the figure, the result of analysis of surface properties is shown as a value histogram of the same sample image elements.

As it follows from detail AFM-image analysis, $Bi_2Te_{3-x}Se_x\langle Ag\rangle$ surface (0001) consists of two sorts of nanofractals. These nanofragments consist of silver chalcogenides and silver particles. The nanofractal size range is within 138 and 69 nm, accordingly, i.e. smaller sizes (~69 nm) belong to Ag. It follows from the histogram (Fig. 4) that ledge size range is within 4-8 nm; the maximal number of particles ($N = 3800$) has $h = 6$ nm height. The distribution function of roughness on a $Bi_2Te_{3-x}Se_x\langle Ag\rangle$ surface along z axis of the sample is more or less homogeneous.

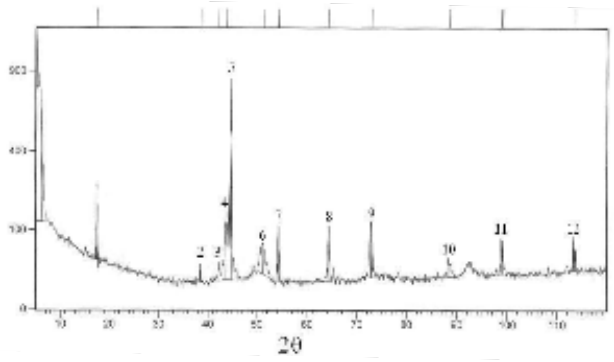

Fig. 1. X-ray diffractometer record of $Bi_2Te_{3-x}Se_x\langle Ag\rangle$ (x = 0.04) crystal surface (0001). *1* – Bi_2Te_3; *2* – Ag, Bi_2Te_3, Ag_2Te, BiTe; *3* – Bi_2Te_3, Ag_2Te; *4* – Ag, Bi_2Te_3, Ag_2Te, BiTe; *5* – Bi_2Te_3, Ag_2Te; *6* – Ag_2Te; *7* – Ag; *8* – Bi_2Te_3, BiTe; *9* – Bi_2Te_3, Ag_2Te; *10* – Ag_2Te, BiTe; *11* – Ag_2Te, BiTe.

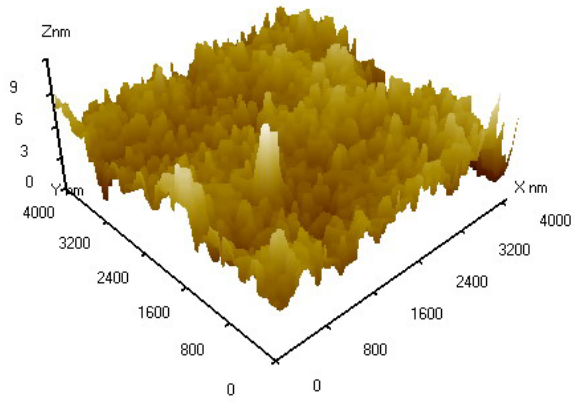

Fig. 2. AFM-image of $Bi_2Te_{3-x}Se_x\langle Ag\rangle$ (x = 0.04) crystal surface (0001) in 3D scale.

The particle distribution function, i.e. its Fourier transform, is shown in Fig. 5. This function shows the distribution of particles with identical sizes. Presence of distinguished wavevectors in the Fourier transform argues the existence of the nanoparticles with typical scale (distance between fractals) in initial image, where this ordering appears.

The comparison of revealed interlaminar fractal images with known structures [3, 4] showed their significant similarity. The nanofractal interlaminar doped surfaces between $Te^{(1)}$–$Te^{(1)}$ in $Bi_2Te_{3-x}Se_x\langle Ag\rangle$ (Fig. 5) are similar to landscapes, constructed by the Voss algorithm [3]. If all the points are transformed by the same way, then this procedure results in self-affine surfaces. The images of surface horizontal sections, obtained by us, are similar to known structures with the fractal dimension $D = 2 - H$. These sections are similar to fractal Brownian lines with $D = 1.5$. These surfaces consisting of infinite number of layers are usually called as Brownian surfaces. This has to do with the fact that any vertical section of this surface looks like a curve typical for the Brownian movement. This surface on the average satisfies the similarity relation and has $H = 3 - D = 0.5$.

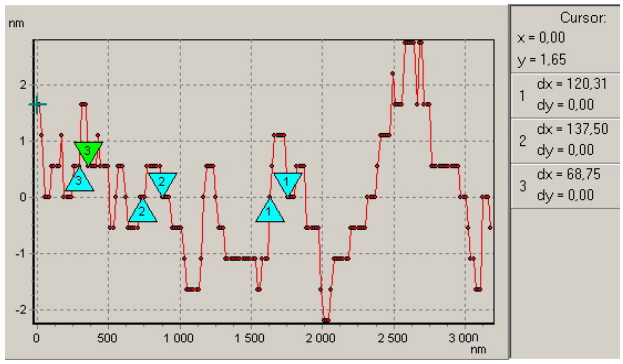

Fig. 3. Relief of $Bi_2Te_{3-x}Se_x\langle Ag\rangle$ (x = 0.04) crystal surface (0001) (along x axis the scanning area is represented by $dx \approx 100$ nm).

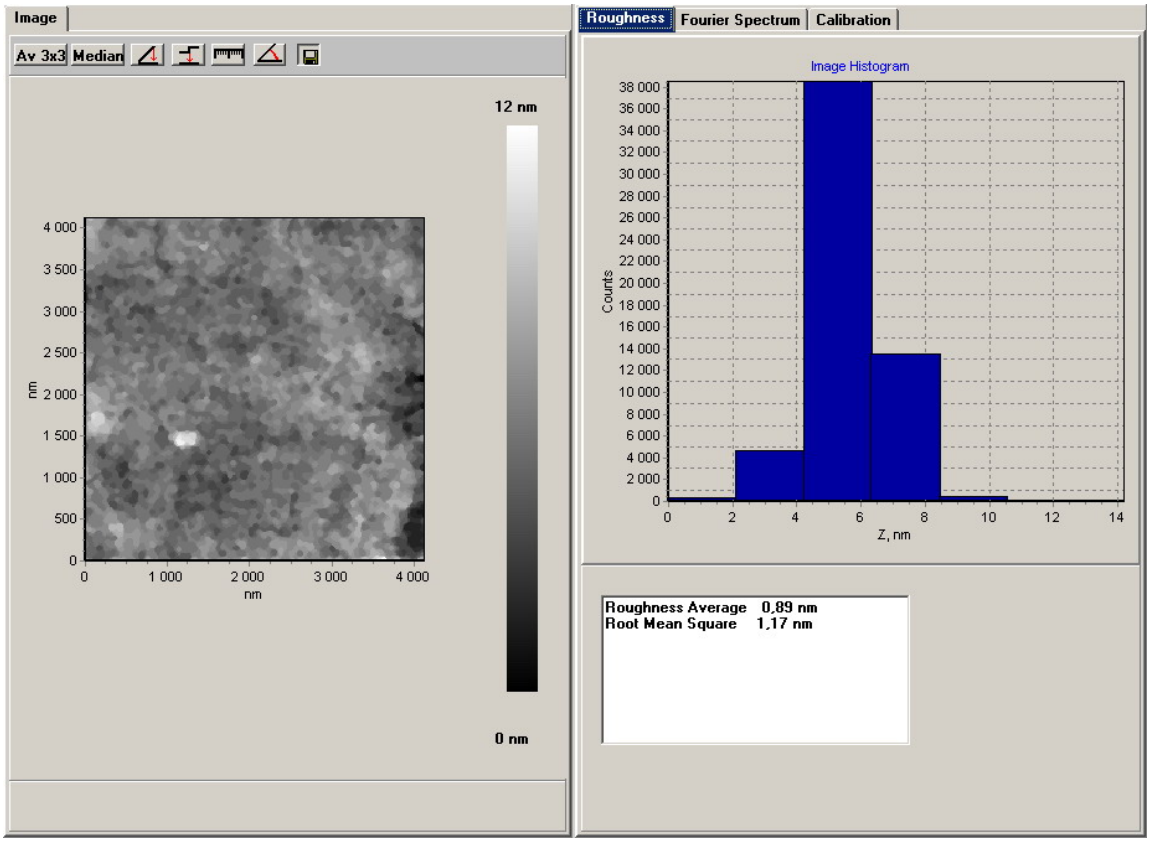

Fig. 4. AFM-image of $Bi_2Te_{3-x}Se_x\langle Ag\rangle$ (x = 0.04) crystal surface (0001) in 2D scale (histogram is in the right corner).

For fractal surfaces represented by us in Fig. 2, as well as for all known similar self-affine fractals, the local and global fractal dimensions should be distinguished. In the case $D > 2$ (in this example $D_{surf} = 2.5$), we have a local surface dimension (D_{surf}).

Let us consider the surfaces inside interlaminar spaces where doped fractal structures are formed (Fig. 2). If on one of the obtained landscapes we cut horizontal section off, then we shall have images as "island" and "coastlines". The fractal dimension of these lines obtained by surface section with a plane makes $D = 2 - H = 1.5$. The nonintegral value $(1 < D < 2)$ argues the flat fractal structure.

In the theory of fractals, there are three types of dimension connected with a self-affine surface: surface dimension D_{surf}, which is local self-affine surface, profile dimension D_{pr}, which is also local and self-affine, contour dimension D_c, which is a self-similar dimension. These fractal dimensions are related to each other by the ratio: $D_{pr} = D_c = D_{surf} - 1$. For $D_c = D_{surf} - 1 = 2.5 - 1 = 1.5$. The obtained experimental data (Figs. 2-5) argue that $Bi_2Te_{3-x}Se_x\langle Ag\rangle$ single crystals are characterized by fractal structures. These fractal structures can be considered as objects with disordered structure "immersed" into Euclidean space of $Te^{(1)}$–$Te^{(1)}$ layers of $Te_{3-x}Se_x\langle Ag\rangle$, and structure objects are perpendicularly directed to a basic plane (0001).

The nature of fractal structure formation on a free surface and inside interlaminar space of $Bi_2Te_{3-x}Se_x\langle Ag\rangle$, $Bi_2Te_3\langle Cu\rangle$, $Bi_2Te_3\langle Ni\rangle$, $Bi_2Te_3\langle B\rangle$, $Bi_2Te_3\langle Sn\rangle$, $Bi_2Te_3\langle Cd\rangle$, $Bi_2Te_3\langle In\rangle$, $Sb_2Te_3\langle Se\rangle$, $Sb_2Te_3\langle Cd\rangle$ layered crystals is similar. The fractal structure of these crystals appears in distribution properties of doped layers between $Te^{(1)}$–$Te^{(1)}$ telluride quintets. For these layers, the following situation is realized: fractal structure properties appear within the scale range bounded below by ~(5-10) nm size, forming a fractal aggregate, and bounded above by the initial fractal cluster size (1000 nm).

The data for $D = 2.5$ structures are comparable with results [2] by the fractal dimension of (particles) clusters formed in a solid particle association.

In the aggregation model [2-4] characterizing the Brownian movement subject to particle cluster, it is accepted that the associating particles are in diffusion spatial motion. I.e., the particle free path in this case is small in comparison with characteristic dimensions of area responsible for fractal growth. The experimental data for mean values of fractal dimensions in a particle association in three-dimensional space (in the model of Brownian movement aggregation) gave the value $D = 2.46 \pm 0.05$ and $D = 1.68 \pm 0.02$ for two-dimensional space.

In the model of fractal cluster growth on a substrate, when cluster sprouts under solid particle

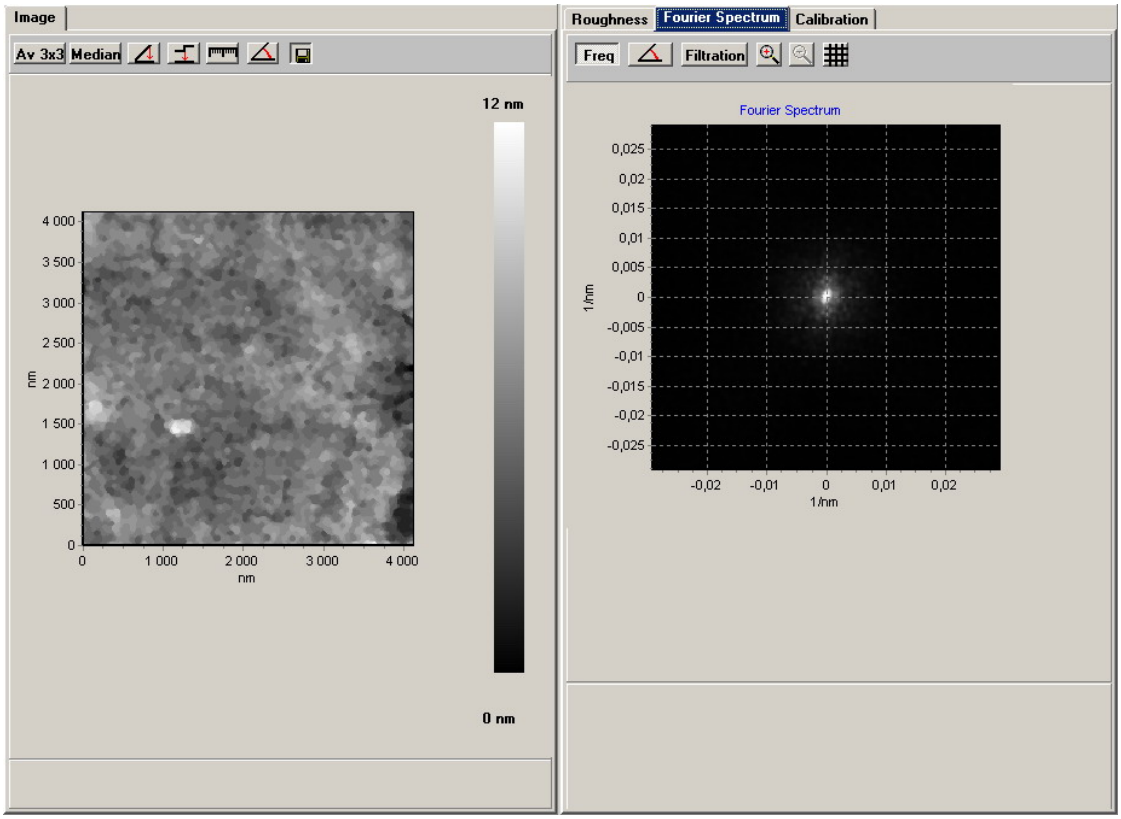

Fig. 5. Distribution function of particles with identical sizes (Fourier transforms).

adhesion to a substrate [3], it is accepted that, growing three-dimensional cluster is formed on a flat substrate. In this case, the crosscut cluster size is significantly less than substrate sizes, and attached particles execute a spatial motion, i.e., clusters sprout from a plane.

According to another model [4], the formed cluster is similar to "wood" of separate "whiskers", sprouting from a plane. In this case, the growth mode is considered, when cluster growth from a plane is possible only in perpendicular direction to a plane, and clusters look like a "sticks". These structures are considered for fractal landscapes obtained by the Voss algorithm.

In crystals based on Bi_2Te_3, the characters of bond between atoms in one layer and between layers are various. The bonds between $Te^{(1)}$–$Te^{(1)}$ telluride quintets are realized by van der Waals type forces, while inside $Te^{(1)}$–$Te^{(1)}$ quintets the ion-covalent forces are prevailing. The principal cause, resulting in cleavage of layered crystals based on Bi_2Te_3 under mechanical loads, is weakness of interlaminar bonds.

On plane surfaces (0001) of crystals based on Bi_2Te_3 (Fig. 2) under investigation, it is possible to notice the presence of forming nanolayers and different size islet traces on them. The nanolayer formation in crystals based on Bi_2Te_3 can be related with draining of diffusing doped atoms (silver, copper and small amounts of nickel) from $Te^{(1)}$–$Te^{(1)}$ telluride quintets and other defects inside interlayers.

The draining periods of doped atoms occur stage by stage: at the first stage the number of passed atoms is not enough and they occupy a small part of interlayer surface. I.e., the doped atoms concentrate in a small amount. With the lapse of time, their concentration reaches the saturation; being merged into nanoparticles they form nanoislets. The process consists of continuous layer formation, on which the finite-size islets concentrate. The total islet amount significantly decreases as a consequence of discrete diffusion particle displacement on short distances, which results in islet merging into one large islet. At the next stage of layer growth, the interlaminar space, in particular $Bi_2Te_{3-x}Se_x\langle Ag\rangle$, gets the greater part of Ag atoms from telluride quintets. The process reaches its peak when islets contact with each other with narrowed tips and merge into conglomerates without total merging. As a result, the fractal cluster formation should occur, forming as a result of particle association subject to the diffusion character of their movement.

4. Conclusions

It follows from experimental data that the obtained fractal structures of $Bi_2Te_{3-x}Se_x\langle Ag\rangle$ crystals have various sizes at the expense of initiation time fluctuation. The beginning of peak formation occurs

after their basis formation mainly on telluride quintets. At the output of vacancy islet surface, diffusion with Ag atom output on a plane (0001) occurs, too, which enlarges and raises the heights of forming fractals. The similar situation can be reflected on AFM 3D images in fractal structure formation depending on atomic radii of dopants (for example, Cu and Ni). Thus, as a result of growth of particle sizes between $Te^{(1)}$–$Te^{(1)}$ layers in $Bi_2Te_{3-x}Se_x\langle Ag\rangle$ the gradual growing fractal structures are formed, filling of which results in fractal surface formation on a basic plane (0001). On a crystal surface (0001), the nanocrystals are formed sooner by self-organization and create visual nanofractal assemblages covering all the $Bi_2Te_{3-x}Se_x\langle Ag\rangle$ basic surface (0001). In connection with nanostructure formation in semiconductors, the fractal nanostructures with large sizes (> 20–25 nm) obtained by us can cause a practical interest due to the influence on properties of semiconductor crystals.

References

1. F.K. Aleskerov, S.K. Kahramanov, E.M. Derun, Some features of formation of nanoobjects in interlayer space of crystals such as Bi_2Te_3 // *Fizika. J. National Acad. Sci. Azerbaijan*, Baku, p. 41-47 (2007).
2. H.E. Hurst, R.P. Black, V.M. Simaika, *Long-Term Storage: An Experimental Study*. Pergamon, London, 1965, p. 230.
3. B.M. Smirnov, *Physics of Fractal Clusters*. Nauka, Moscow, 1991, p. 192 (in Russian).
4. P. Meakin, Fractal structures // *Progress in Solid State Chemistry* **20** (3), p. 135-233 (1990).